Single-layer multiband infrared metallodielectric photonic crystals designed by genetic algorithm optimization

Robert P. Drupp, Jeremy A. Bossard, Douglas H. Werner, and Theresa S. Mayer[a)]
Department of Electrical Engineering, Center for Nanoscale Science, The Pennsylvania State University, University Park, Pennsylvania 16802

(Received 3 September 2004; accepted 4 January 2005; published online 14 February 2005)

Metallodielectric photonic crystals (MDPCs) consisting of a planar periodic array of metallic patch elements designed by genetic algorithm (GA) optimization were patterned on flexible dielectric substrates and exhibit strong mid- and far-infrared (IR) dual-band response. The GA uses biological principles of natural selection to evolve nonintuitive geometries by optimizing the MDPC scattering response based on a user-defined fitness function. The transmission spectra measured on two different MDPCs optimized for optically thin and thick substrates have two strong stop bands with attenuation greater than 10 dB, which agree well with those predicted by full-wave periodic method of moments (PMM) modeling. This versatile GA optimization approach will facilitate design of scaled mid- and near-IR MDPCs with user-defined scattering response. © *2005 American Institute of Physics*. [DOI: 10.1063/1.1868884]

Metallodielectric photonic crystals (MDPCs) have been the subject of considerable interest recently for the scientifically fascinating and technologically attractive optical properties they exhibit. For example, light transmission has been observed through one-dimensional photonic crystals (PCs) comprised of alternating layers of metal and dielectric when the total metal thickness is many times the skin depth.[1,2] In two dimensions, periodic arrays of metal nanoparticles placed on a dielectric that supports guided optical modes have been used to suppress light extinction within the particle-plasmon resonance.[3,4] Finally, infrared (IR) filters that have one or more resonant transmission stop or pass bands have been demonstrated using two- and three-dimensional MDPCs.[5–11]

Recently, we designed single-layer IR MDPCs that had dual-band transmission response with strong band rejection ($>$10 dB) using a full-wave periodic method of moments (PMM) model and exploiting the self-similar geometry of fractal metallic patch elements.[10] The excellent agreement between the spectra predicted by PMM simulations and measured experimentally on fractal MDPCs with the same geometry show that PMM modeling accurately determines the scattering response of such structures. However, the geometrical constraints associated with fractal MDPCs impose limitations in design flexibility, which include the ability to tailor the design for specific stop-band positions, angular dependence of the incident radiation, and arbitrary substrate thickness. In this letter, we report on the implementation and experimental verification of a versatile design technique that employs genetic algorithm (GA) optimization to create user-defined MDPCs with nonintuitive metallic element geometries that exhibit strong dual-band IR transmission responses in a single-layer structure.

GAs have been used previously as an effective optimization technique for designing microwave antennas and frequency selective surfaces.[12,13] The ability to optimize many variables simultaneously also makes this approach well suited for designing MDPCs. In this optimization procedure, biological principles of natural selection are used to find a solution with an approximate global maximum of a user-defined fitness function.[14] The GA explores a large solution space by randomly generating an initial population of solutions where all the variable parameters of each solution are encoded in a binary string or chromosome. The fitness of each solution in the population is evaluated and "parents" are chosen; solutions with the highest fitness have the best chance of being selected. A crossover operator is then used to splice the parents' chromosomes to generate "offspring" for a next generation population with characteristics that are derived from the naturally selected parents. As shown in the flowchart in Fig. 1, the process continues over many generations until a solution that meets the specified fitness value is determined.

The GA optimization was implemented by representing the pixels that comprise one unit cell of the periodic metal patch element pattern as a binary string where each binary state indicates the presence ("1") or absence ("0") of metal on a given pixel. The pixel size was fixed by the minimum resolution that could be achieved during MDPC fabrication, and the unit-cell size was included in the chromosome as a

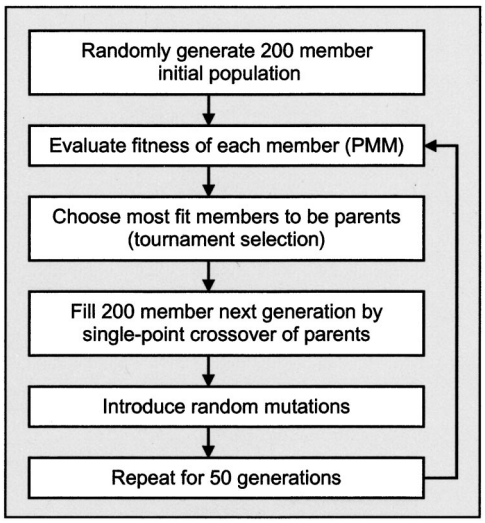

FIG. 1. Flowchart of the GA used for MDPC design.

[a)]Electronic mail: tsm2@psu.edu

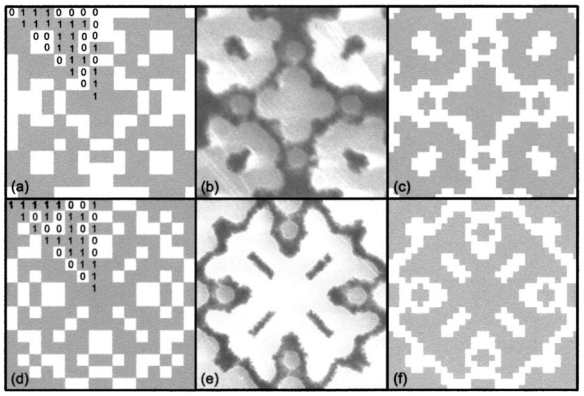

FIG. 2. (a) GA-optimized unit cell with overlaid chromosome values of the MDPC designed for a 0.5 μm polyimide substrate with stop bands at 23 and 43 μm. (b) SEM image of the fabricated MDPC. (c) Modeled geometry trimmed to the fabricated MDPC. (d)–(f) Corresponding process for the MDPC designed for a 4 μm thick polyimide substrate with stop bands at 38 and 75 μm.

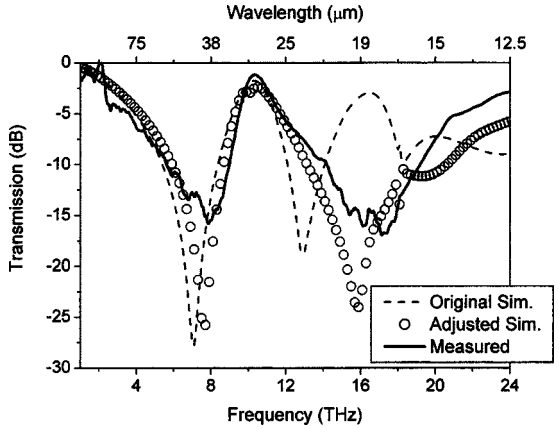

FIG. 3. Transmission spectra of GA-optimized MDPC designed for a 0.5 μm thick polyimide substrate with stop-bands at 23 and 43 μm. The dashed curve shows the response of the original design optimized by the GA [Fig. 2(a)] with stop bands at the requested positions. The solid curve is the measured response of the fabricated structure [Fig. 2(b)]. The circles show the modeled response after the metal patch elements are trimmed to match the fabricated structure [Fig. 2(c)]. The modeled spectra include dielectric and metallic losses.

variable parameter. Eight-fold symmetry was applied to the unit cell to ensure polarization insensitivity of the final structure. The fitness of each possible solution was evaluated by comparing the PMM-calculated scattering response with the desired response described by the fitness function given by

$$\text{Fitness} = \frac{1}{\sum_{\text{stop bands}} P_{\text{trans}} + \sum_{\text{pass bands}} P_{\text{refl}}}, \tag{1}$$

where P_{trans} and P_{refl} are the transmittance and reflectance, which are both maximized over the desired stop and pass bands of the MDPC.

We verified the validity of this GA-based optimization design approach by creating a dual-band IR MDPC with a transmission response similar to that of the two-stage fractal structures studied previously.[10] The fitness function was selected to reward reflection for normally incident radiation at the two desired stop-band wavelengths of 23 and 40 μm, and transmission at the remaining wavelengths of 10–100 μm over which the optimization was performed. For the initial study, the dielectric substrate on which the aluminum metal elements were defined was a polyimide film with a fixed thickness of 0.5 μm, which is optically thin (i.e., less than 1/20 of the shortest resonant wavelength) and has very good IR transparency in the wavelength regime of interest. The design optimization was conducted using published values of wavelength dependent metallic loss[15] and an approximate wavelength independent substrate effective permittivity of $\varepsilon_r = 3.0 - 0.3_j$.[16] Although this design was optimized for normally incident radiation, it should be noted that this approach also facilitates designs where the spectral response of the MDPC can be optimized for arbitrary angles of incident radiation. Moreover, in more sophisticated designs, the substrate thickness and permittivity can be optimized or selected from a table of available dielectric materials by the GA.

One unit cell of the MDPC produced by this GA design optimization strategy is shown in Fig. 2(a), which includes the binary representation of each pixel overlaid on one of the eight symmetric folds. It measures 23.2×23.2 μm^2 and has 16×16 pixilation. The simulated transmission spectrum of the MDPC is shown by the dashed curve in Fig. 3, and contains two strong stop bands (>15 dB) at the requested wavelengths of 23 and 40 μm.

The MDPC was fabricated by patterning a 1 cm^2 periodic array of the unit cell on top of a 0.5 μm thick polyimide substrate, which was deposited by spin coating onto a silicon wafer that served as a mechanical support. The metal elements were defined using conventional optical lithography followed by liftoff of a 75 nm thick layer of thermally evaporated aluminum. Prior to spectral characterization, the silicon immediately beneath the MDPC active area was removed by selective etching in sodium hydroxide. The as-designed MDPC unit cell required slight geometrical modifications (i.e., trimming) to facilitate pattern transfer using optical lithography, which included separating and/or removing adjacent metal pixels that touched only at their corners. This is illustrated in the scanning electron microscope (SEM) image of a fully fabricated unit cell shown in Fig. 2(b). Transmission spectra of these structures were collected with the sample at normal incidence to the IR beam using a Bruker Optics Equinox 55 Fourier transform infrared spectrometer and normalized to the background of the substrate.

The measured transmission spectrum is shown by the solid curve in Fig. 3, and contains two stop bands centered at 17 and 39 μm each with attenuation greater than 15 dB. While there is good correspondence between the modeled and measured stop band centered at 40 μm, the second stop band is shifted significantly to shorter wavelengths. This is a result of differences in unit-cell geometry introduced by pattern trimming and transfer. To verify this, the pixilation of the unit cell of the modeled MDPC was increased to 32×32 to produce a pattern that more accurately represents the as-fabricated structure illustrated in Fig. 2(c). The modeled transmission spectrum that takes these differences into account is shown as the open circles in Fig. 3. As is evident from this comparison, there is very good agreement between the modeled and measured transmission spectra when the unit-cell geometries of the modeled and fabricated structures are nearly identical, and metallic and dielectric loss is included in the model. The most significant deviation between the two spectra is noted at shorter wavelengths, and can likely be attributed to the use of a wavelength independent complex permittivity in the model.

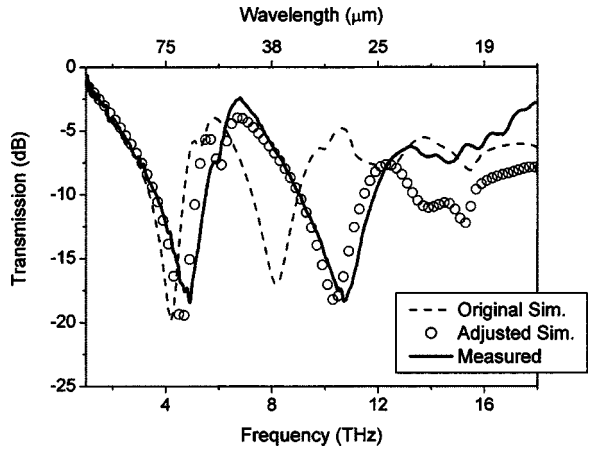

FIG. 4. Transmission spectra of GA-optimized MDPC designed for a 4 μm thick polyimide substrate with stop bands at 38 and 75 μm. The dashed curve shows the response of the original design optimized by the GA [Fig. 2(d)] with stop bands at the requested positions. The solid curve is the measured response of the fabricated structure [Fig. 2(e)]. The circles show the modeled response after the metal patch elements are trimmed to match the fabricated structure [Fig. 2(f)]. The modeled spectra include dielectric and metallic losses.

For many applications, it is advantageous for the substrate to be mechanically flexible and of sufficient strength that it can be readily removed from the sacrificial wafer used during processing. To accomplish this, we investigated designs that use thicker 4 μm polyimide substrates. It should be noted that MDPC designs based on more conventional resonant patch elements typically have one or more spurious stop bands due to the presence of standing waves in the substrate when the dielectric substrate is not optically thin. The GA-based design can overcome this limitation by optimizing over a large solution space such that spurious stop bands are penalized in the fitness function and are consequently minimized. This was investigated by designing a MDPC for a 4 μm thick substrate with stop bands specified at 38 and 75 μm for normally incident radiation using GA optimization over the 27–100 μm wavelength range. One unit cell of the MDPC designed to meet these requirements is shown in Fig. 2(d). The modeled transmission spectrum for this design that accounts for material losses is shown as the dashed curve in Fig. 4 and has strong stop bands centered at 37 and 71 μm, which are nearly identical to the requested stop-band positions. A SEM image of the as-fabricated trimmed unit cell for this design is shown in Fig. 2(e).

The transmission spectrum of the MDPC was measured at normal incidence after it was removed from the sacrificial silicon wafer. As shown by the solid curve in Fig. 4, the fabricated MDPC has two stop bands with attenuation of approximately 18 dB centered at 28 and 61 μm. As noted previously for the thin 0.5 μm substrate MDPC design, the stop-band positions are shifted considerably to 28 and 61 μm from the designed positions of 38 and 75 μm. The modeled response determined using a modified unit cell that more accurately reflects the geometry of the as-fabricated trimmed structure [Fig. 2(f)] is given as open circles in Fig. 4. This demonstrates the excellent correspondence between the measured and modeled MDPC spectra for wavelengths greater than 25 μm, where the wavelength independent dielectric permittivity incorporated into the model satisfactorily accounts for substrate loss. In the future, the wavelength dependent complex dielectric permittivity of each substrate will be measured using IR spectroscopic ellipsometry and incorporated into the model to further improve the accuracy of the GA design optimization procedure.

In conclusion, single-layer dual-band IR MDPCs that are comprised of a periodic array of metallic patch elements designed by GA optimization were investigated theoretically and experimentally. This design technique uses biological principles of natural selection to optimize the PMM-modeled scattering response based on a user-defined fitness function, which allows greater flexibility when compared to designs that use simple resonant patch elements. We verified the validity of this approach by designing and implementing dual-band MDPCs that were optimized for specific stop bands on optically thin and thick (0.5 and 4.0 μm) polyimide substrates. In both cases, there was very good agreement between the modeled and measured transmission spectra when geometrical factors and material loss were considered. Moreover, the attenuation in all of the transmission stop bands exceeded the targeted value of 10 dB required for most high performance applications. These design methodologies will facilitate further scaling of the MDPCs into the mid- and near-IR wavelength regime using advanced nanolithographic techniques, such as imprint lithography.[17] Future work is aimed at investigating these scaled structures as well as incorporating geometrical design rules into the GA optimization routine to produce MDPC designs that account for the practical constraints imposed on the patch elements during fabrication.

This research was supported by the NSF MRSEC, Center for Nanoscale Science, Grant No. DMR-0213623. One of the authors (R. D.) acknowledges support from a Materials Research Institute Graduate Fellowship. The authors also acknowledge the Penn State Materials Characterization Laboratory for SEM facilities.

[1] M. Scalora, M. J. Bloemer, A. S. Pethel, J. P. Dowling, C. M. Bowden, and A. S. Manka, J. Appl. Phys. **83**, 2377 (1998).
[2] M. J. Bloemer and M. Scalora, Appl. Phys. Lett. **72**, 1676 (1998).
[3] S. Linden, J. Kuhl, and H. Geissen, Phys. Rev. Lett. **86**, 4688 (2001).
[4] V. Yannopapas and N. Stefanou, Phys. Rev. B **69**, 012408 (2004).
[5] J. S. McCalmont, M. M. Sigalas, G. Tuttle, K.-M. Ho, and C. M. Soukolis, Appl. Phys. Lett. **68**, 2759 (1996).
[6] S. Gupta, G. Tuttle, M. Sigalas, and K.-M. Ho, Appl. Phys. Lett. **71**, 2412 (1997).
[7] I. Pascau, W. L. Schaich, and G. D. Boreman, Appl. Opt. **40**, 118 (2001).
[8] H. A. Smith, M. Rebbert, and O. Sternberg, Appl. Phys. Lett. **82**, 3605 (2003).
[9] J. A. Oswald, B.-I. Wu, K. A. McIntosh, L. J. Mahoney, and S. Verghese, Appl. Phys. Lett. **77**, 2098 (2000).
[10] R. P. Drupp, J. A. Bossard, Y.-H. Ye, D. H. Werner, and T. S. Mayer, Appl. Phys. Lett. **85**, 1835 (2004).
[11] K. A. McIntosh, L. J. Mahoney, K. M. Molvar, O. B. McMahon, S. Verghese, M. Rothschild, and E. R. Brown, Appl. Phys. Lett. **70**, 2937 (1997).
[12] R. Haupt and S. Haupt, *Practical Genetic Algorithms* (Wiley, New York, 1997).
[13] S. Chakravarty and R. Mittra, IEEE Trans. Electromagn. Compat. **44**, 338 (2002).
[14] J. M. Johnson and Y. Rahmat-Samii, IEEE Antennas Propag. Mag. **39**, 7 (1997).
[15] A. Rakic, A. Djurisic, J. Elazar, and M. Majewski, Appl. Opt. **37**, 5271 (1998).
[16] Z. M. Zhang, G. Lefever-Burton, and F. R. Powell, Int. J. Thermophys. **19**, 905 (1998).
[17] T. C. Bailey, S. C. Johnson, S. V. Sreenivasan, J. G. Ekerdt, C. G. Willson, and D. J. Resnick, J. Photopolym. Sci. Technol. **15**, 481 (2002).